Heliyon 10 (2024) e40108

Contents lists available at ScienceDirect

Heliyon

journal homepage: www.cell.com/heliyon

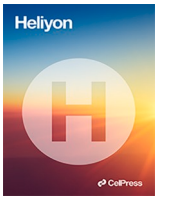

Research article

Antibacterial and antibiofilm features of *mut*SMAP-18 against *Vibrio cholerae*

Ishrat Jahan [a], Byambasuren Ganbaatar [b], Chul Won Lee [b], Sung-Heui Shin [a,c], Sungtae Yang [a,c,d,*]

[a] *Department of Biomedical Sciences, School of Medicine, Chosun University, Gwangju, 61452, Republic of Korea*
[b] *Department of Chemistry, Chonnam National University, Gwangju, 61186, Republic of Korea*
[c] *Department of Microbiology, School of Medicine, Chosun University, Gwangju, 61452, Republic of Korea*
[d] *Institute of Well-Aging Medicare & CSU G-LAMP Project Group, Chosun University, Gwangju, 61452, Republic of Korea*

ARTICLE INFO

Keywords:
Vibrio cholerae
Antimicrobial peptide
SMAP-18
Antibiofilm

ABSTRACT

Cholera continues to be a pointed global health issue, prominently in developing nations, where the disease's severe diarrheal symptoms pose substantial public health risks. With the escalating spread of antibiotic resistance among *V. cholerae* strains, alternative therapeutic approaches are imperative. Antimicrobial peptides are increasingly recognized for their potential, with research focusing on finding the most effective options. We explored the antibacterial and antibiofilm properties of analogues of sheep myeloid antimicrobial peptide-18 (SMAP-18) against *V. cholerae* in this investigation. Our prior research demonstrated that substituting glycine with alanine at different positions within SMAP-18 altered its structure and antimicrobial activity. Among these altered analogues, our focus was on a mutant variant (*mut*SMAP-18), characterized by glycine-to-alanine substitutions at positions 2, 7, and 13. Our results indicated that *mut*SMAP-18 exhibited heightened antimicrobial and antibiofilm activities against *V. cholerae* compared to SMAP-18. We conducted several mechanistic investigations to check the membrane integrity using DNA-binding dye, SYTOX Green or measuring calcein dye leakage and analyzing flow cytometry by fluorescence-activated cell sorting (FACScan). From these tests, we elucidated that SMAP-18 primarily functions intracellularly, while *mut*SMAP-18 targets the bacterial membrane. Additionally, scanning electron microscopy (SEM) images illustrated membrane disruption at lower concentrations for *mut*SMAP-18. Notably, *mut*SMAP-18 demonstrated significant antibiofilm properties against *V. cholerae*. Overall, these findings offer valuable perspectives for developing novel antibacterial therapies targeting the pathogenic *V. cholerae*.

1. Introduction

Cholera, a centuries-old infectious disease, has sparked seven pandemics over the past two centuries [1,2]. While predominantly affecting developing countries, the World Health Organization (WHO) warns about persistent risk of outbreaks spreading to non-endemic regions [1–4]. Characterized initially by watery diarrhea, cholera rapidly progresses to severe dehydration and, without immediate intervention, can result in death. The culprit behind this fatal diarrheal disease is *Vibrio cholerae*. The virulence of

* Corresponding author. Department of Biomedical Sciences, School of Medicine, Chosun University, Gwangju, 61452, Republic of Korea.
E-mail address: styang@chosun.ac.kr (S. Yang).

https://doi.org/10.1016/j.heliyon.2024.e40108
Received 18 August 2024; Received in revised form 31 October 2024; Accepted 1 November 2024
Available online 2 November 2024

V. cholerae can vary, with strains classified as either pathogenic or nonpathogenic based on their genetic makeup. In regard to its somatic (O) antigens, choleragenic *V. cholerae* is divided into two serogroups. Strains of *V. cholerae* that react with polyvalent O1 antiserum are in serogroup O1, while those that do not are classified as serogroup non-O1. Known as serogroup O139, the non-O1*V. cholerae* strains are agglutinable by their own particular antisera. Even if non-O1/non-O139 serogroups might rarely make people sick, they have not developed into epidemic strains [2,3]. Notably, the toxigenic serogroups O1 and O139 pose significant threats for causing epidemic or endemic disease [2,3,5]. The pathogenic *V. cholerae* enters the small intestine after passing through the gastric acid barrier, where they colonize, multiply, and start secreting cholera toxin. To develop severe cholera, a significant infectious dose of roughly 10^8 bacteria is required [6,7]. Without proper treatment, cholera can quickly worsen, with mortality rates possibly reaching 50 % within a matter of hours to a few days following the onset of symptoms [8]. Treatment typically involves oral or intravenous rehydration therapy to restore lost fluids and electrolytes. Antibiotics are often recommended in conjunction with rehydration therapy, aiming to decrease the severity of symptoms, shorten the length of illness, and reduce bacterial shedding, thereby minimizing the risk of transmission. The combination of rehydration and antibiotics ensures both immediate symptom relief and a reduction in the overall disease burden [3,7,9]. Traditionally, tetracyclines and fluoroquinolones have been widely used as antibiotics for cholera treatment, aimed at alleviating the symptoms [10,11]. However, there has been a notable increase in the prevalence of *V. cholerae* strains exhibiting resistance to the usual conventional antibiotics, leading to major epidemics in several geographical regions [12,13]. Although the primary treatment for cholera is still rehydration therapy, the rise of antibiotic-resistant strains has prompted interest in exploring alternative therapeutic options to complement current interventions. Despite the rapid development and widespread adoption of newer generations of antibiotics, even the most potent antimicrobial agents have proven inadequate in mitigating the morbidity and mortality associated with antimicrobial resistance (AMR) [14,15]. A recent study estimates that approximately 4.95 million deaths worldwide in 2019 were attributable to bacterial AMR, solidifying its status as one of the foremost global health threats [16,17]. The escalating challenge of AMR underscores the urgent need for novel therapeutic strategies to combat the relentless rise of antibiotic-resistant pathogens.

Antimicrobial peptides (AMPs), owing to their reduced susceptibility to bacterial resistance mechanisms, have become a potential class of compounds under investigation to combat multi-drug resistant bacteria, demonstrating encouraging outcomes over conventional antibiotics [18–22]. AMPs can fight against multiple types of microorganisms including bacteria, viruses, and fungi, rendering them as promising new antibiotic candidates. Animal studies have corroborated the antibacterial effectiveness of AMPs, with cathelicidins demonstrating the ability to limit bacterial infections and prevent death in infected mouse models when administered [23,24]. Found in sheep white blood cells, Sheep Myeloid Antimicrobial Peptide-29 (SMAP-29) is a cathelicidin-type antimicrobial peptide containing 29 amino acids. This peptide demonstrates wide-ranging antimicrobial properties, effectively targeting multiple pathogens including bacteria, fungi, and viruses [25–27]. Researchers have explored various approaches to develop analogues with reduced toxicity while maintaining potent antimicrobial activity since the original peptide can damage red blood cells and is toxic to mammalian cells [26–32]. The structural features of SMAP-29 reveal an amphipathic α-helical region in the N-terminal residues (1-18), while the C-terminal residues (19–29) possess hydrophobic characteristics responsible for its hemolytic activity. Previous studies have demonstrated that the truncated N-terminal region, comprising residues 1–18 and referred to as SMAP-18, exhibits effective antimicrobial activity with reduced toxicity compared to the parent peptide [26–28,30,33]. The development of SMAP-18, a truncated variant of SMAP-29, preserves its antimicrobial potency, thereby suggesting it could be valuable for future research and possible medical treatments.

The antimicrobial peptide SMAP-18 includes four glycine (Gly) residues positioned at the 2nd, 7th, 13th, and 18th positions in its sequence. It is noteworthy that Gly18, located at the C-terminus, is not projected to significantly influence the structural characteristics of the peptide. Glycine is known for its greater conformational flexibility compared to other amino acids and can act as a disruptor of helical structures. Our recent study has revealed that substituting glycine residues with alanine (Ala) in SMAP-18 can induce alterations in its structural conformation, thereby affecting its mechanism of action. Replacing Gly with Ala (specifically G2A, G7A, G13A, G7,13A, and G2,7,13A) has minimal impact on the antimicrobial activities of SMAP-18, however, mutations at Gly7 and Gly13 resulted in a change in the mechanism of action [33]. The introduction of alanine substitutions at glycine residues 7 and 13 in SMAP-18, resulting in the mutant peptide *mut*SMAP-18 designated with the sequence RALRRLARKIAHAVKKYG, has been shown to modulate the structural conformation and, consequently, the mode of action of SMAP-18. In this study, we investigate whether *mut*SMAP-18 exhibits effective antimicrobial activity against *V. cholerae*. By exploring the potential of *mut*SMAP-18 to combat this pathogen, we aim to gain insights that may contribute to the development of novel therapeutic strategies tailored to combat cholera and other infections caused by *V. cholerae*.

2. Materials and methods

2.1. Peptide synthesis and bacterial strain

As outlined in our prior study, peptides have been synthesized [33]. In summary, both SMAP-18 peptides were produced using a solid-phase synthesis method that employed 9-fluorenylmethoxycarbonyl (Fmoc) chemistry on rink amide 4-methylbenzhydrylamine (MBHA) resin. As coupling agents, N,N′-diisopropylcarbodiimide (DIC) and hydroxybenzotriazole (HOBt) were used in conjunction with protected amino acids in this procedure. Peptides were then cleaved from the resin with a mixture of trifluoroacetic acid (TFA), water, ethanedithiol, phenol and thioanisole. The raw peptides were purified via preparative reverse-phase high-performance liquid chromatography (RP-HPLC) on a Shim-pack C18 column, and their purity, confirmed to exceed 95 %, was verified using analytical RP-HPLC and electrospray ionization (ESI)-LC–MS.

V. *cholerae* strain (ATCC 14035) was used in this study. This strain is a member of the O1 serogroup, which causes most cholera outbreaks globally. It was initially cultured on Mueller–Hinton agar plates with 1 % NaCl and incubated at a temperature of 37 °C for 24 h. One bacterial colony was selected for inoculation on 5 mL of Mueller–Hinton broth having 1 % NaCl which was then incubated at 37 °C with agitation at 180 rpm for the entire night. This culture was diluted further and incubated until it reached the stationary phase. This culture with an optical density (OD_{600}) of 0.5 was used as a stock for the following experiments.

2.2. Determination of minimum inhibitory concentrations (MICs)

In accordance with the recommendations provided by CLSI, we tested the peptides' antimicrobial efficacy against *V. cholerae* [34]. To establish minimum inhibitory concentrations (MICs), we utilized the microtiter broth dilution technique. The bacterial culture was grown overnight in Mueller–Hinton broth supplemented with 1 % NaCl, maintaining temperature at 37 °C until they reached the stationary phase. The cultures were then incubated further to reach mid-log phase, indicated by an OD_{600} reading of 0.5. Dilutions of these cultures were prepared in the same broth medium and were distributed into 96-well plates where various concentrations of the test peptides had been serially diluted. After overnight incubation was completed at 37 °C, MIC values were determined by identifying the lowest peptide concentration at which bacterial growth was inhibited, as measured by a microplate ELISA reader at 600 nm wavelength.

2.3. SYTOX green uptake assay

Membrane permeabilization on *V. cholerae* induced by our peptides was assessed through the SYTOX Green uptake assay in the mid-log phase, as described previously [35]. The culture underwent three washes with 1 × PBS and diluted to reach an OD_{600} at 0.07. A bacterial suspension of $\sim 10^6$ CFU/ml was prepared following the washing process and was mixed with 0.5 μM SYTOX Green, after which it was incubated for 15 min under dark conditions. SYTOX Green uptake was monitored after peptides were added at 1 × MIC concentration, using a Shimadzu RF-5300PC fluorescence spectrophotometer. The measurements were conducted at excitation and emission wavelengths of 485 nm and 520 nm, respectively. Melittin was utilized as a positive control in this assay.

2.4. Calcein dye leakage assay

Large unilamellar vesicles (LUVs) with entrapped calcein were prepared following an established prptocol [36]. For liposome construction, egg yolk phosphatidylethanolamine (EYPE) and egg yolk phosphatidyl-DL-glycerol (EYPG) were combined in a 1:1 M ratio to mimic the bacterial cell membrane. The lipids were first dissolved in chloroform, after which they were dried. The following day, the dried lipids were resuspended in a 70 mM calcein solution. The resulting suspension was subjected to vortexing for 4–5 h, followed by 10–12 cycles of rapid heating and cooling. The mixture was then extruded 21 times through a LiposoFast-Extruder fitted with 100 nm pore size filters. Entrapped calcein was separated by gel filtration using a Sephadex G-50 column. Calcein leakage from liposomes was monitored with or without peptides using a Shimadzu RF-5300PC fluorescence spectrophotometer, where excitation and emission wavelengths were set at 490 nm and 520 nm, respectively. The peptides were added at their corresponding MICs and melittin was employed as a control peptide in the experimental procedure.

2.5. FACScan analysis

The integrity of bacterial cell membranes was assessed through flow cytometry analysis, where propidium iodide (PI) uptake was quantified using a FACScan instrument in accordance with established protocols [37]. *V. cholerae* cells in the mid-log phase were diluted to reach an OD_{600} absorbance of approximately 0.5. A mixture was made when equal volumes of cell suspension and PBS (1 ×) were combined, after which centrifugation was performed at 8000 rpm for 5 min. Following PBS removal, the cell pellets were resuspended in fresh PBS. PI (10 μL) was then introduced and was allowed to incubate for 15 min. The peptides, at concentrations equivalent to their MICs, were added to the suspension, and a further 15-min incubation period was implemented. Melittin, a peptide targeting the membrane, was employed as the control peptide. The PI fluorescence was then measured by a FACScan machine and compared with the fluorescence of bacteria with no peptide.

2.6. Scanning electron microscopy (SEM)

Scanning Electron Microscopy (SEM) was employed to examine the membrane morphology of *V. cholerae* (ATCC 14035) in the presence of SMAP-18 and *mut*SMAP-18. The bacteria were spread on Mueller–Hinton agar plate (1 % NaCl) and left to grow overnight at 37 °C. One specific bacterial colony was chosen to incubate again into Mueller–Hinton broth (with 1 % NaCl) for entire night at 37 °C with agitation at 180 rpm. When the strains attained the optical density (OD600) of 0.5, it was then diluted in the same culture media to an OD_{600} of 0.1. Each peptide was added to achieve concentrations equivalent to 2 × MIC and 4 × MIC, and the cell suspension was then incubated at a maintained temperature of 37 °C with a 4-h duration. The peptide melittin which is capable of membrane disruption served as a positive control. For SEM visualization, the specimens were mounted onto aluminum stubs and were subjected to gold coating under vacuum conditions. Microscopic examination was subsequently performed by using a Gemini 500 + EDS SEM following the manufacturer's specifications.

2.7. Biofilm inhibition & biofilm eradication

To assess the efficacy of our peptide analogues against *V. cholerae* biofilm, we investigated both biofilm inhibition and biofilm eradication, following procedures outlined previously [37–39]. Bacteria were cultured to logarithmic phase in MHB plus 1 % NaCl and then incubated at a temperature of 37 °C with peptides that were serially diluted. A multi-functional peptide, LL-37 which has significant antibiofilm property was utilized as the control peptide [40]. Absorbance measurements at 600 nm were recorded for final analysis, and graphs were constructed using SigmaPlot software. Biofilm eradication assessment was conducted utilizing 96-well Calgary microtiter plates containing PEG, where bacterial cells were initially cultured at a temperature of 37 °C and then treated with different concentrated peptides (serially diluted). Upon completion of the incubation period, the plate lids were subjected to cleaning with PBS to get rid of any planktonic bacteria and air-drying. Subsequently, bacterial fixation was achieved using methanol treatment, after which crystal violet staining was implemented for 5 min. Following the removal of the excess staining solution, 95 % ethanol was introduced into the wells, and agitation was maintained for 30 min. Spectrophotometric measurements were obtained at 600 nm wavelength, and the resultant data were processed through SigmaPlot software for graphical representation.

2.8. Light microscopic image analysis for V. cholerae biofilms

Our peptides' biofilm-disruptive efficacy against *V. cholerae* was assessed through a light microscopy using crystal violet staining. First, *V. cholerae* cells were allowed to form biofilms over a 48-h incubation period. After biofilm formation, the peptides (SMAP-18 and mutSMAP-18) were introduced at varying concentrations (1 x, 2 x, and 4 x MICs) and incubated for an additional 24 h. Subsequently, the planktonic cell suspension was carefully discarded, and the remaining biofilms were undergone with gentle PBS washing. The biofilm fixation was done with methanol, afterwards 0.5 % crystal violet solution was introduced for a duration of 15 min. Following the removal of excess stains, the stained biofilms were examined under a light microscope for visual assessment of biofilm integrity and disruption.

2.9. Confocal laser scanning microscopy (CLSM)

Evaluating the viability of bacteria in response to the peptides, we conducted confocal laser scanning microscopy (CLSM) following similar procedures as reported previously [37]. Biofilm formation was facilitated by incubating mid-log phase *V. cholerae* cultures in 6-well plates with coverslips containing MHB (1 % NaCl supplementation) at 37 °C for a 48-h duration. The cellular specimens were subsequently subjected to PBS washing procedures, whereupon fluorescent staining was implemented utilizing a Bacterial Viability kit (Invitrogen) in accordance with manufacturer specifications. The dual nucleic acid staining components, SYTO-9 and propidium iodide (PI), were administered to the specimens, followed by a 30-min dark incubation period. Post-incubation, excess staining reagents were eliminated through washing procedures, and methanol fixation was performed. Following air-drying, the coverslips were mounted onto microscopic slides. Untreated biofilm specimens were maintained as experimental controls. Biofilm mass visualization and quantification were conducted utilizing confocal laser-scanning microscopy (Zeiss Microscopy), and subsequent image analysis was ensured using ZEN 2009 Light Edition software.

2.10. Statistical analysis

The statistical evaluation and graphical representations were performed using a combination of SPSS 16.0 and SigmaPlot v12.0 software packages, employing one-way ANOVA. All results are presented as mean values with standard deviation, based on three separate experimental runs. Statistical significance was evaluated through the Mann-Whitney *U* test.

3. Results

3.1. Characterization of peptides

Reverse-phase high-performance liquid chromatography (RP-HPLC) and electrospray ionization-mass spectrometry (ESI-MS) methods were used to verify that the actual molecular weights of the synthesized SMAP-18 and mutant SMAP-18 (*mut*SMAP-18) peptides matched their predicted molecular weights. Using internet resources, the physicochemical characteristics of both peptides were computed including net charge, hydrophobicity and hydrophobic moment (the amphipathicity or structural distribution of

Table 1
Amino acid sequences and physicochemical properties of SMAP-18 and *mut*SMAP-18.

Peptides	Amino acid sequence	Molecular Mass (g/mol)	Net charge	Hydrophobicity[a]	Hydrophobic moment (μH)[b]
SMAP-18	RGLRRLGRKIAHGVKKYG	2064.3	+7	0.045	0.614
*mut*SMAP-18	RALRRLARKIAHAVKKYG	2106.3	+7	0.097	0.633

[a] Hydrophobicity and.
[b] Hydrophobic moment (μH) were computed via internet at: https://heliquest.ipmc.cnrs.fr/cgi-bin/ComputParams.py (accessed on March 15, 2024).

hydrophobic residues). Specifically, the helical wheel projections (Fig. S1) were generated via the HeliQuest server to visualize these characteristics (Table 1). Both SMAP-18 and mutSMAP-18 were found to be cationic (positively charged) peptides, but they exhibited differences in their hydrophobicity values.

3.2. Antibacterial activity

The antibacterial action of SMAP-18 and the mutant analog (*mut*SMAP-18) against *V. cholerae* was determined in terms of their minimum inhibitory concentrations (MICs), which represent the lowest concentrations necessary to inhibit bacterial growth. *V. cholerae* requires a saline environment with concentrations ranging from 0.25 % to 3 % for optimal growth [41,42]. Prior to applying salt media to *V. cholerae*, we assessed the efficacy of the peptides in NaCl-containing media. Initially, we tested the peptide analogues on a common gram-negative bacterium, *E. coli*, in salt media and observed that the antimicrobial activity of *mut*SMAP-18 remained consistent across varying NaCl concentrations (Table S1). Consequently, we selected 1 % NaCl-MHB media for the antimicrobial experiments involving SMAP-18 peptides against *V. cholerae*. MIC values for SMAP-18 and *mut*SMAP-18 against *V. cholerae* were 16 μM and 8 μM, respectively (Table 2). In comparison, the control peptide melittin exhibited an MIC of 2 μM against the same bacterial strain. Notably, SMAP-18 and *mut*SMAP-18 were relatively non-toxic at concentrations higher than their respective MICs, as assessed by cytotoxicity assays on mouse macrophage RAW 264.7 cells (Fig. S2). Both peptides exhibited approximately 80 % cell viability in RAW 264.7 cells when tested at four times higher concentration than their MICs (4 × MICs).

3.3. Antimicrobial mechanism

To elucidate the mechanisms of action of SMAP-18 and its mutant form against *V. cholerae*, three different assays were performed: SYTOX Green uptake, calcein dye leakage, and flow cytometry analysis. SYTOX Green uptake assay measures the ability of SYTOX Green, a fluorescent dye that binds to DNA, to enter bacterial cells upon membrane permeabilization. As seen in Fig. 1A, SMAP-18 have not significantly elevated fluorescence intensity compared to the membrane-targeting peptide melittin at its minimum inhibitory concentration (MIC). In contrast, *mut*SMAP-18 caused a considerable increase in fluorescence intensity, suggesting membrane permeabilization. Liposomes that resembled bacterial cell membranes were used in a calcein dye leakage test to further validate the membrane-targeting mechanism of *mut*SMAP-18. The liposomes were prepared with a 1:1 M ratio of EYPE and EYPG lipids. Treatment with *mut*SMAP-18 resulted in higher fluorescence intensity, similar to the effect observed with melittin, indicating dye leakage due to membrane disruption (Fig. 1B).

Additionally, flow cytometry analysis using a FACScan was employed to assess the membrane integrity and quantify the membrane-lytic effects of the peptides on *V. cholerae* (Fig. 2). A DNA-binding dye known as propidium iodide (PI) indicated the membrane disruption caused by the peptides. Without any peptide treatment (Fig. 2A), no shift in fluorescence was found in the control sample, indicating intact bacterial membranes. However, when treated with *mut*SMAP-18 or the membrane-targeting peptide melittin (Fig. 2B), more than 60 % of the bacterial population exhibited a fluorescence shift at 1 × MIC, suggesting significant membrane disruption. In contrast, SMAP-18 treatment (Fig. 2C) resulted in an insignificant fluorescence shift compared to *mut*SMAP-18 (Fig. 2D) and melittin. These findings suggest that *mut*SMAP-18 functions as a membrane-targeting peptide, causing membrane permeabilization and disruption, whereas SMAP-18 appears to exert its antimicrobial activity through an intracellular mode of action without significantly compromising the bacterial membrane integrity.

Finally, a visual comparison of the morphological changes in *V. cholerae* cells with or without SMAP-18 peptides was performed using scanning electron microscopy (SEM). Fig. 3 illustrates the SEM images of this pathogen at a magnification of 25000×. Untreated cells exhibited intact bacterial membranes, whereas compromised membranes were observed in the presence of peptides. Upon exposure to SMAP-18 at 4 times its minimum inhibitory concentration (4 × MIC), membrane damage was evident, but only minor morphological changes were observed at 2 × MIC. In contrast, treatment with *mut*SMAP-18 caused significant disruption of the bacterial cells, even at 2 × MIC. At 4 × MIC, *mut*SMAP-18 induced a level of cell death comparable to that caused by melittin, suggesting complete membrane disruption and cellular disintegration.

Table 2
Minimum concentrations requirement for antimicrobial and antibiofilm activity against *Vibrio cholerae*.

	Antimicrobial and antibiofilm activity (μM)		
Peptides	MICs[a]	MBICs[b]	MBECs[c]
SMAP-18	16	16	64
*mut*SMAP-18	8	8	32
Melittin	2	2	ND[d]

[a] Minimum inhibitory concentrations (MICs) were defined as the minimal concentration of the antimicrobial agent that constrained microbial growth.
[b] Minimum biofilm inhibitory concentrations (MBICs) were termed as the lowest concentration of the antimicrobial agent that inhibited the biofilms formed by microbes.
[c] Minimum biofilm eradication concentrations (MBECs) were stated as the lowest possible concentration of the antimicrobial agent required to effectively eradicate or eliminate pre-formed bacterial biofilms.
[d] ND: Not determined.

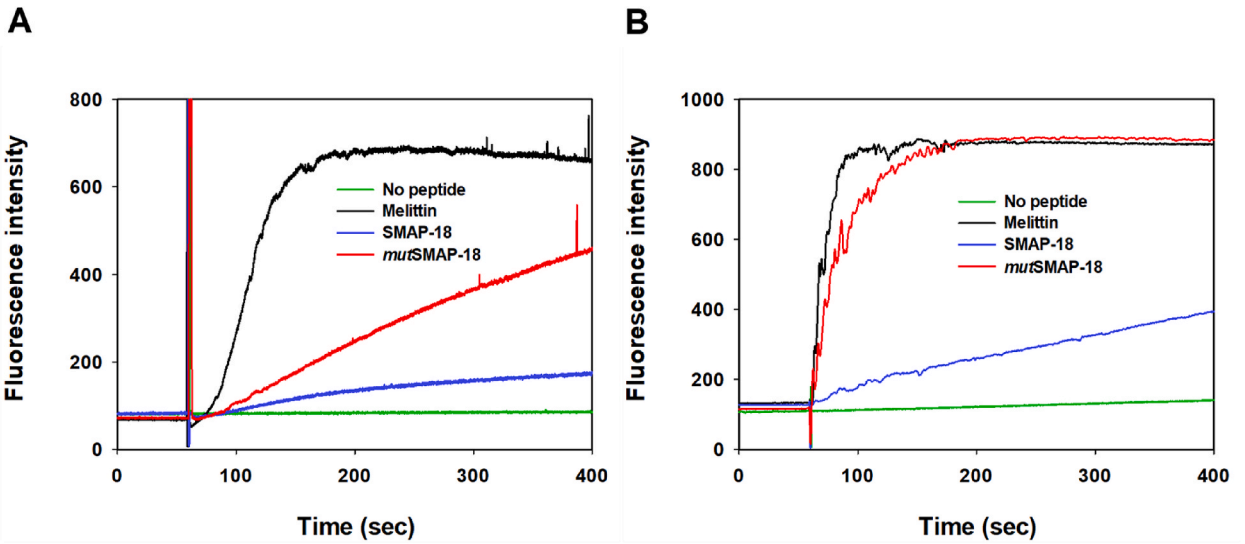

Fig. 1. Mechanism study of SMAP-18 peptides on *Vibrio cholerae*; (A) SYTOX green uptake assay of SMAP-18 peptides on *V. cholerae* at 1 × MIC; (B) Calcein dye leakage (EYPE: EYPG = 1:1) assay of SMAP-18 peptides on *V. cholerae* at 1 × MIC.

3.4. Antibiofilm activity

Our peptides' antibiofilm capabilities against *V. cholerae* were assessed by in vitro biofilm inhibition and eradication experiments, which were also observed using light microscopy and confocal laser scanning microscopy (CLSM) (Fig. 4). The results unequivocally demonstrated the superior antibiofilm activity of *mut*SMAP-18 in comparison to SMAP-18 (Fig. 4A and B). In Table 2, the minimum biofilm inhibitory concentrations (MBICs) were found to be 16 μM for SMAP-18 and 8 μM for *mut*SMAP-18. Notably, the minimum biofilm eradication concentrations (MBECs) were determined to be 64 μM and 32 μM for SMAP-18 and *mut*SMAP-18, respectively, which are four times higher than their corresponding MICs.

For light microscopic observations (Fig. 4C), three different peptide concentrations (1 × , 2 × , and 4 × MICs) were evaluated, with untreated biofilms serving as the control. The images revealed significant biofilm inhibition at 2 × MICs and successful eradication at 4 × MIC upon treatment with *mut*SMAP-18. Additionally, CLSM imaging (Fig. 4D), utilizing propidium iodide (PI) and SYTO-9 dyes to differentiate between dead and live cells, respectively, demonstrated a higher proportion of dead cells within the biofilms after exposure to *mut*SMAP-18, further corroborating its potent antibiofilm effects.

4. Discussion

Diverse approaches have been proposed to improve antimicrobial peptides' (AMPs) therapeutic efficacy. These methodologies encompass structural modifications targeting core motifs or specific amino acid substitutions, elimination of hydrophobic residues, modulation of helical conformations, and conjugation with cell-penetrating peptides. Such interventions have demonstrated augmented antimicrobial potency coupled with improved cell selectivity, thereby mitigating cytotoxicity concerns [43–48]. In our prior investigation, we also employed diverse strategies to identify the most efficacious SMAP-29 analogue. Our findings revealed that single amino acid substitutions in an 18-mer SMAP resulted in variations in both the antibacterial activity as well as mechanism of action. Particularly, the substitution of glycine with alanine at positions 2, 7, and 13, designated as *mut*SMAP-18, stabilized the helical structure, thereby enhancing antimicrobial efficacy against a wide range of common bacterial strains. Although truncation generally resulted in diminished antimicrobial activity, *mut*SMAP-18 exhibited a pronounced bactericidal effect against *Escherichia coli, Salmonella typhimurium, Pseudomonas aeruginosa, Bacillus subtilis, and Staphylococcus aureus* except *Staphylococcus epidermidis*, suggesting strain-specific susceptibility [33].

The primary target of this study is to explore the antibacterial and anti-biofilm effects of SMAP-18 analogues against *V. cholerae*. Even though it has historically been common, this pathogen still poses a serious risk to global public health as it can trigger endemic outbreaks. According to the WHO, cholera has re-emerged as a disease of global importance, manifesting in regions where it had been previously absent for an extended period [9]. The rise of resistance to traditional antibiotics in developing countries has become a concerning issue [12,13,49,50], underscoring the urgent need to explore alternative therapeutic strategies to combat future cholera outbreaks. In this context, several approaches have been undertaken to develop therapeutic alternatives against multi-drug resistant pathogens, including the development of novel antimicrobial peptides with enhanced cell selectivity [46,51–53]. Recent studies on antimicrobial peptides have demonstrated promising results against *Vibrio* species in both laboratory and in animal models [22,49,54]. Especially, bovine lactoferrin and its derivatives have exhibited effectiveness against multidrug-resistant strains of *Vibrio* species in animal models [22]. Additionally, an in vivo study reported that granulysin derivative peptides have notable antibacterial activity

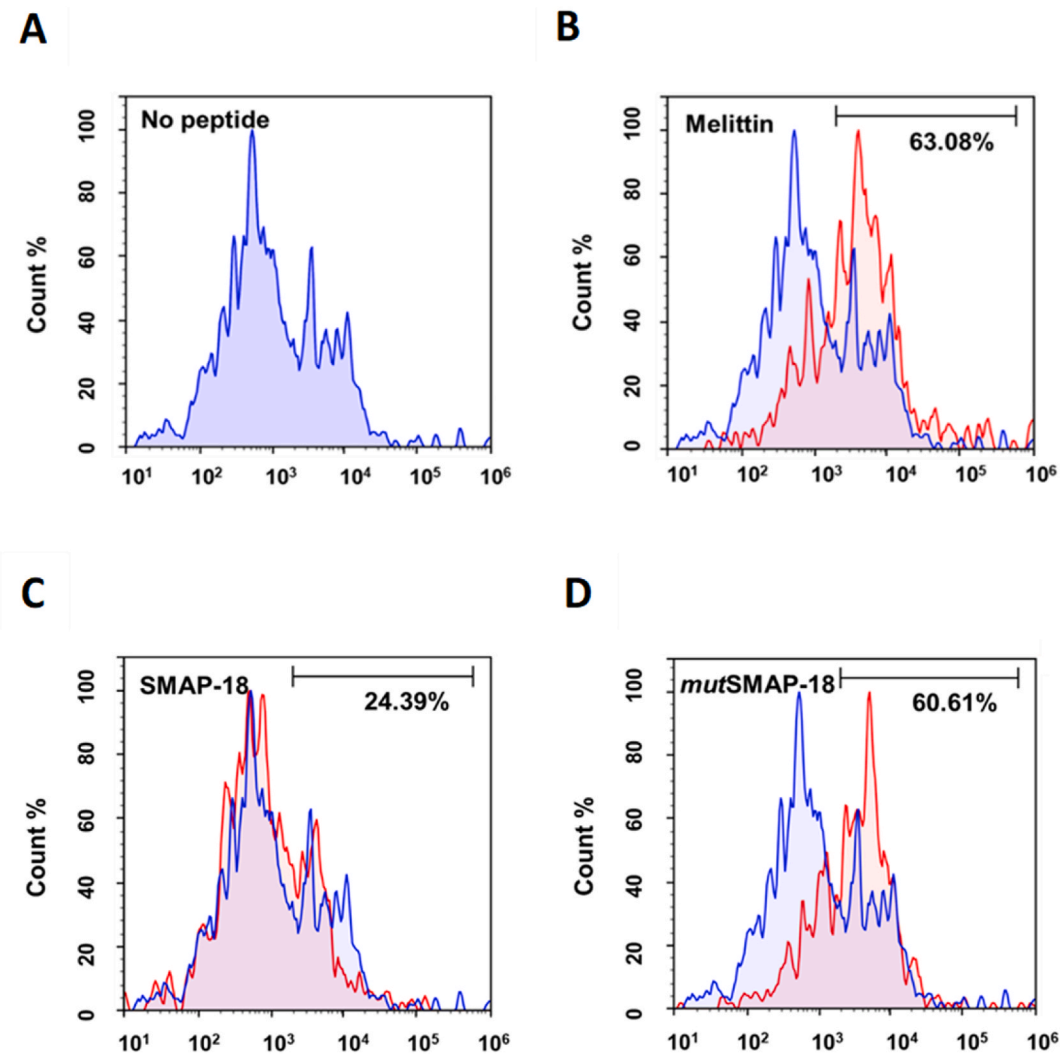

Fig. 2. Membrane integrity disruption of *Vibrio cholerae* in the absence (A) and presence of peptides: (B) melittin, (C) SMAP-18 and (D) *mut*SMAP-18 at 1 × MIC, measured by an increase in the fluorescent intensity of propidium iodide (PI).

against *V. cholerae* [49]. In the present study, we focus on the N-terminal (1-18) fragment of SMAP-29, termed SMAP-18, and its analogue against *V. cholerae*, as SMAP-18 has previously demonstrated cell selectivity against various pathogens [28,30,31].

Our study demonstrated that both SMAP-18 and the alanine-substituted analogue *mut*SMAP-18 exhibited effective inhibitory effects on the *V. cholerae* within the tested concentration of 16 μM (Table 2). Notably, *mut*SMAP-18 displayed a bacteriostatic effect at a MIC one-fold lower than that of SMAP-18. This differential potency suggests that the two peptides may exert their antimicrobial actions through distinct mechanisms. To elucidate the antibacterial mechanisms of SMAP-18 and *mut*SMAP-18 against *V. cholerae*, we performed a series of mechanistic studies, including the SYTOX Green uptake assay, calcein dye leakage test, and flow cytometry analysis (Figs. 1 and 2). Collectively, the results of these experiments indicated that SMAP-18 exerts its antimicrobial effects through an intracellular mode of action, whereas *mut*SMAP-18 functions as a membrane-targeting agent. These results align with our earlier research investigating the mechanisms of action of these peptides against other pathogenic bacteria [33]. Scanning electron microscopy (SEM) imaging further corroborated the membrane-disruptive effects of *mut*SMAP-18 on *V. cholerae* cells. SMAP-18, on the other hand, appeared to cause less severe membrane damage at lower concentrations, indicating a potentially different mechanism of action. The SEM images revealed complete disruption and damage to the bacterial cell membranes upon exposure to *mut*SMAP-18, exhibiting a pattern similar to that observed with the membrane-targeting peptide melittin (Fig. 3). However, in contrast to the cytotoxic nature of melittin and the parent peptide SMAP-29, the truncated analogues SMAP-18 and *mut*SMAP-18 demonstrated significantly lower cytotoxicity, with over 50 % mammalian cell viability observed at concentrations as high as 128 μM (Fig. S2). Although previous research has suggested that SMAP-18 may act intracellularly in certain pathogens, we cannot rule out the possibility that both SMAP-18 and *mut*SMAP-18 share similar membrane-targeting mechanisms against *V. cholerae*, with varying efficiencies. Further mechanistic analyses are required for complete clarification of the precise modes of action of both SMAP-18 and *mut*SMAP-18.

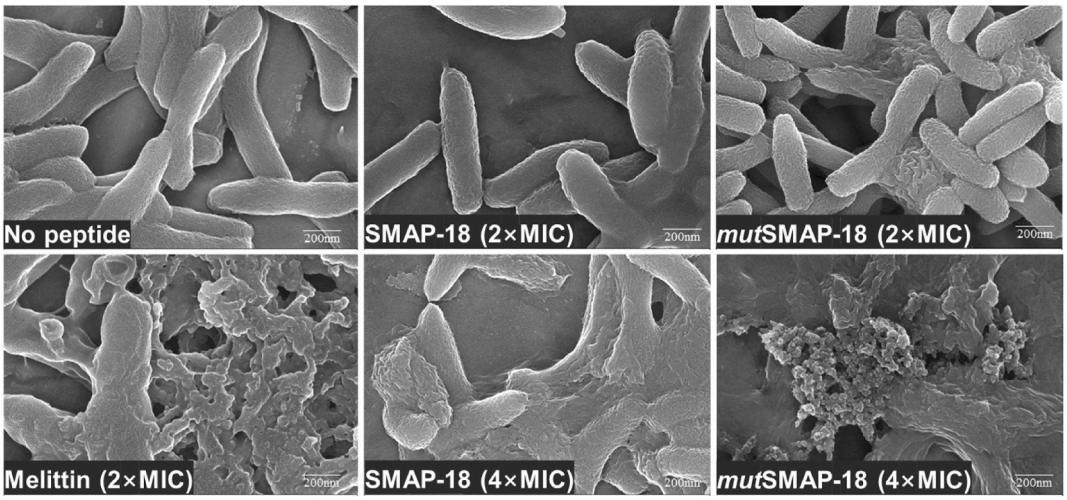

Fig. 3. Scanning electron microscopy (SEM) showing morphological changes of *Vibrio cholerae* in presence of peptides with different concentrations. The scale bar was 200 nm.

V. cholerae, the causative agent of cholera, utilizes biofilm formation as an important survival strategy during its aquatic and intestinal life cycle phases, conferring resistance to environmental stresses and increasing infectivity [55,56]. *V. cholerae* biofilm is formed in a complex, multifaceted way; controlled by an intricate network of transcriptional factors, signaling molecules, and environmental cues [57–59]. We evaluated the antibiofilm properties of SMAP-18 and *mut*SMAP-18 against *V. cholerae* biofilms, which is pivotal for the pathogenicity and environmental persistence of this organism. Our results revealed that *mut*SMAP-18 exhibited superior antibiofilm activity compared to SMAP-18, as evidenced by its lower minimum biofilm eradication concentration (MBEC) (Fig. 4). Images from light microscopy and confocal laser scanning microscopy also evidenced its effective antibiofilm features. As the antibiotic resistance is most common in biofilm-forming bacteria, our synthesized *mut*SMAP-18 peptide may lead to development of a new antibiofilm agent against *V. cholerae.* The overall findings underscore the potential of *mut*SMAP-18 as a promising therapeutic candidate for combating *V. cholerae* infections, owing to its enhanced antimicrobial potency, membrane-targeting mechanism, and antibiofilm effects. Animal studies will be pursued in future research to extend the findings of this work.

5. Conclusion

Considering the resurgence of cholera and the growing risk of antibiotic resistance, our research aims to contribute in developing effective therapeutic interventions against this persistent public health threat. By investigating the antibacterial and antibiofilm properties of SMAP-18 analogues, we seek to generate insights which may inform the design and formulation of novel therapeutic agents to combat cholera and other infections caused by *Vibrio* spp., particularly in the face of emerging antimicrobial resistance.

CRediT authorship contribution statement

Ishrat Jahan: Writing – original draft, Investigation. **Byambasuren Ganbaatar:** Investigation. **Chul Won Lee:** Writing – review & editing, Validation. **Sung-Heui Shin:** Writing – review & editing, Validation. **Sungtae Yang:** Writing – review & editing, Validation, Supervision, Conceptualization.

Data availability

All data were included in the article and Supplements.

Funding

This research was supported by the National Research Foundation of Korea (NRF) grant funded by the Korean government (MSIT) (No. RS-2023-00210292 and No. 2022R1F1A1068595) and the Global-Learning & Academic Research Institution for Master's·PhD students, and Postdocs (LAMP) Program of the National Research Foundation of Korea (NRF) grant funded by the Ministry of Education (No. RS-2023-00285353).

Declaration of competing interest

The authors declare that they have no known competing financial interests or personal relationships that could have appeared to

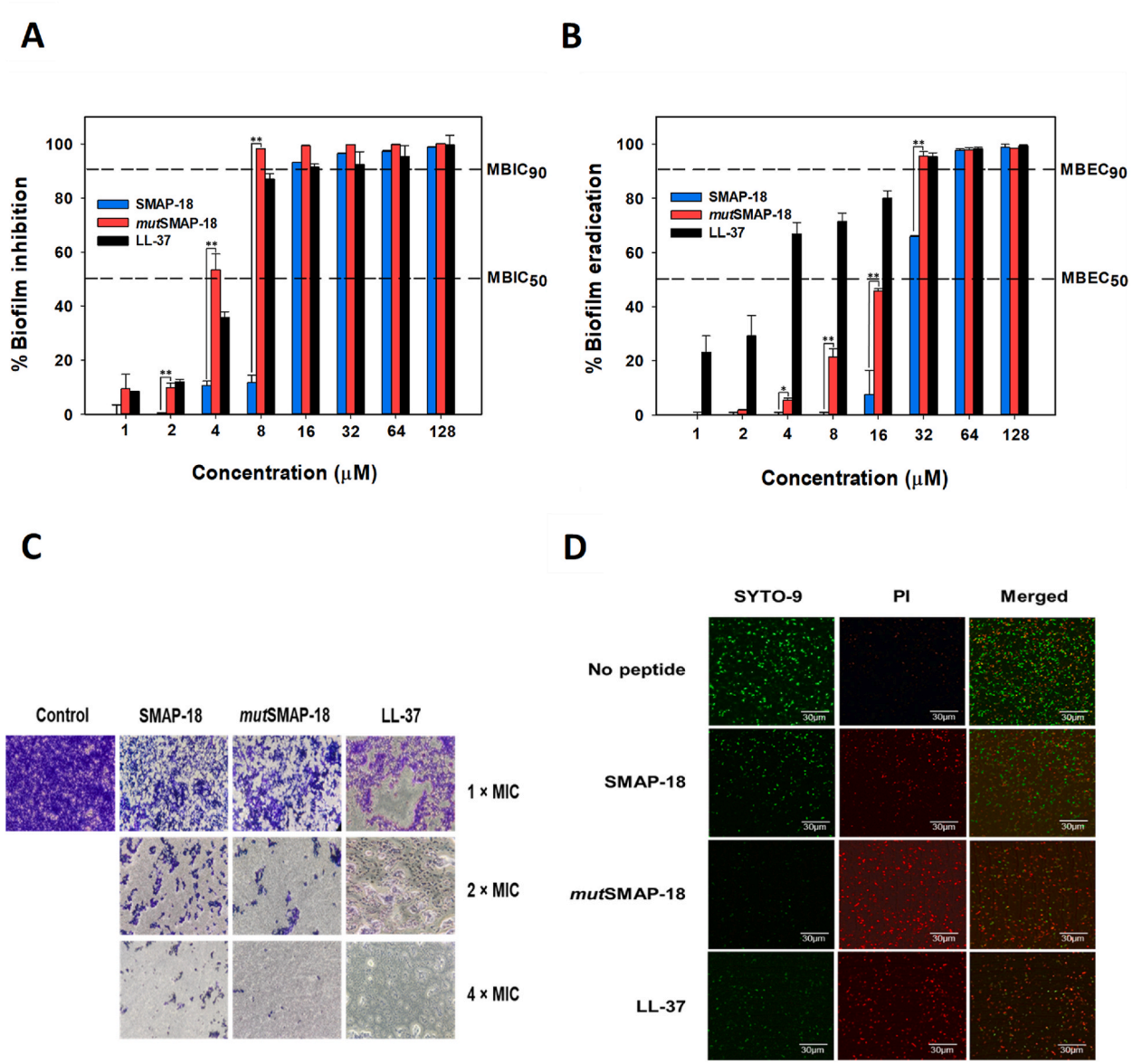

Fig. 4. Antibiofilm activity of SMAP-18 peptides against *Vibrio cholerae*: (A) Biofilm inhibition; (B) Biofilm eradication; The results are presented as the mean ± standard deviation (SD) from three independent experiments, with error bars representing SD. Statistical significance between the two peptides is denoted by *P<0.05 and **P<0.01. (C) Biofilm disruption by peptides under light microscope using crystal violet; (D) Confocal laser scanning microscopy (CLSM) images showing biofilm eradication with a live/dead bacterial viability staining kit (SYTO 9/PI). Live and dead cells are indicated by green fluorescence (SYTO 9) and red fluorescence (PI), respectively. The scale bar was 30 μm.

influence the work reported in this paper.

Appendix A. Supplementary data

Supplementary data to this article can be found online at https://doi.org/10.1016/j.heliyon.2024.e40108.

References

[1] E. Buliva, S. Elnossery, P. Okwarah, M. Tayyab, R. Brennan, A. Abubakar, Cholera prevention, control strategies, challenges and World Health Organization initiatives in the Eastern Mediterranean Region: a narrative review, Heliyon 9 (5) (2023) e15598.

[2] S. Mandal, M.D. Mandal, N.K. Pal, Cholera: a great global concern, Asian Pac. J. Tropical Med. 4 (7) (2011) 573–580.
[3] M.H. Ahmadi, Global status of tetracycline resistance among clinical isolates of Vibrio cholerae: a systematic review and meta-analysis, Antimicrob. Resist. Infect. Control 10 (2021) 1–12.
[4] V. Torane, S. Kuyare, G. Nataraj, P. Mehta, S. Dutta, B. Sarkar, Phenotypic and antibiogram pattern of V. cholerae isolates from a tertiary care hospital in Mumbai during 2004–2013: a retrospective cross-sectional study, BMJ Open 6 (11) (2016) e012638.
[5] D.A. Sack, R.B. Sack, G.B. Nair, A.K. Siddique, Cholera, Lancet 363 (2004) 223–233.
[6] R.A. Cash, S.I. Music, J.P. Libonati, M.J. Snyder, R.P. Wenzel, R.B. Hornick, Response of man to infection with Vibrio cholerae. I. Clinical, serologic, and bacteriologic responses to a known inoculum, J. Infect. Dis. 129 (1) (1974) 45–52.
[7] M. Kitaoka, S.T. Miyata, D. Unterweger, S. Pukatzki, Antibiotic resistance mechanisms of Vibrio cholerae, J. Med. Microbiol. 60 (4) (2011) 397–407.
[8] R.M. Maier, I.L. Pepper, C.P. Gerba, Environmental microbiology, Academic press2009.
[9] W.H. Organization, Oral Rehydration Salts: Production of the New ORS, World Health Organization, 2006.
[10] F. Mhalu, P. Mmari, J. Ijumba, Rapid emergence of El Tor vibrio cholera resistant to antimicrobial agents during first six months of fourth cholera epidemic in Tanzania, Lancet 313 (8112) (1979) 345–347.
[11] K. Towner, N. Pearson, F. Mhalu, F. O'grady, Resistance to antimicrobial agents of Vibrio cholerae El Tor strains isolated during the fourth cholera epidemic in the United Republic of Tanzania, Bull. World Health Organ. 58 (5) (1980) 747.
[12] P. Garg, S. Sinha, R. Chakraborty, S. Bhattacharya, G.B. Nair, T. Ramamurthy, Y. Takeda, Emergence of fluoroquinolone-resistant strains of Vibrio cholerae O1 biotype El Tor among hospitalized patients with cholera in Calcutta, India, Antimicrobial agents and chemotherapy 45 (5) (2001) 1605–1606.
[13] S.K. Kar, B.B. Pal, H.K. Khuntia, K.G. Achary, C.P. Khuntia, Emergence and spread of tetracycline resistant Vibrio cholerae O1 El Tor variant during 2010 cholera epidemic in the tribal areas of Odisha, India, Int. J. Infect. Dis. 33 (2015) 45–49.
[14] D. Longworth, Microbial drug resistance and the roles of the new antibiotics, Cleve. Clin. J. Med. 68 (6) (2001).
[15] B. Spellberg, R. Guidos, D. Gilbert, J. Bradley, H.W. Boucher, W.M. Scheld, J.G. Bartlett, J. Edwards Jr., I.D.S.o. America, The epidemic of antibiotic-resistant infections: a call to action for the medical community from the Infectious Diseases Society of America, Clin. Infect. Dis. 46 (2) (2008) 155–164.
[16] C.J. Murray, K.S. Ikuta, F. Sharara, L. Swetschinski, G.R. Aguilar, A. Gray, C. Han, C. Bisignano, P. Rao, E. Wool, Global burden of bacterial antimicrobial resistance in 2019: a systematic analysis, The lancet 399 (10325) (2022) 629–655.
[17] W.H. Organization, Global antimicrobial resistance and use surveillance system (GLASS) report 2022, World Health Organization2022.
[18] R.E. Hancock, H.-G. Sahl, Antimicrobial and host-defense peptides as new anti-infective therapeutic strategies, Nat. Biotechnol. 24 (12) (2006) 1551–1557.
[19] M. Zasloff, Antimicrobial peptides of multicellular organisms, nature 415 (6870) (2002) 389–395.
[20] K. E Greber, M. Dawgul, Antimicrobial peptides under clinical trials, Current topics in medicinal chemistry 17 (5) (2017) 620–628.
[21] K. Garbacz, W. Kamysz, L. Piechowicz, Activity of antimicrobial peptides, alone or combined with conventional antibiotics, against Staphylococcus aureus isolated from the airways of cystic fibrosis patients, Virulence 8 (1) (2017) 94–100.
[22] E. Acosta-Smith, K. Viveros-Jiménez, A. Canizalez-Román, M. Reyes-Lopez, J.G. Bolscher, K. Nazmi, H. Flores-Villaseñor, G. Alapizco-Castro, M. De la Garza, J. J. Martínez-Garcia, Bovine lactoferrin and lactoferrin-derived peptides inhibit the growth of Vibrio cholerae and other Vibrio species, Front. Microbiol. 8 (2018) 2633.
[23] V. Nizet, T. Ohtake, X. Lauth, J. Trowbridge, J. Rudisill, R.A. Dorschner, V. Pestonjamasp, J. Piraino, K. Huttner, R.L. Gallo, Innate antimicrobial peptide protects the skin from invasive bacterial infection, Nature 414 (6862) (2001) 454–457.
[24] A. Giacometti, O. Cirioni, R. Ghiselli, F. Mocchegiani, G. D'Amato, R. Circo, F. Orlando, B. Skerlavaj, C. Silvestri, V. Saba, Cathelicidin peptide sheep myeloid antimicrobial peptide-29 prevents endotoxin-induced mortality in rat models of septic shock, Am. J. Respir. Crit. Care Med. 169 (2) (2004) 187–194.
[25] B. Skerlavaj, M. Benincasa, A. Risso, M. Zanetti, R. Gennaro, SMAP-29: a potent antibacterial and antifungal peptide from sheep leukocytes, FEBS Lett. 463 (1–2) (1999) 58–62.
[26] S.Y. Shin, E.J. Park, S.-T. Yang, H.J. Jung, S.H. Eom, W.K. Song, Y. Kim, K.-S. Hahm, J.I. Kim, Structure–activity analysis of SMAP-29, a sheep leukocytes-derived antimicrobial peptide, Biochemical and biophysical research communications 285 (4) (2001) 1046–1051.
[27] R.M. Dawson, C.Q. Liu, Cathelicidin peptide SMAP-29: comprehensive review of its properties and potential as a novel class of antibiotics, Drug Dev. Res. 70 (7) (2009) 481–498.
[28] R.M. Dawson, C.-Q. Liu, Analogues of peptide SMAP-29 with comparable antimicrobial potency and reduced cytotoxicity, Int. J. Antimicrob. Agents 37 (5) (2011) 432–437.
[29] R.M. Dawson, J. McAllister, C.-Q. Liu, Characterisation and evaluation of synthetic antimicrobial peptides against Bacillus globigii, Bacillus anthracis and Burkholderia thailandensis, Int. J. Antimicrob. Agents 36 (4) (2010) 359–363.
[30] B. Jacob, Y. Kim, J.-K. Hyun, I.-S. Park, J.-K. Bang, S.Y. Shin, Bacterial killing mechanism of sheep myeloid antimicrobial peptide-18 (SMAP-18) and its Trp-substituted analog with improved cell selectivity and reduced mammalian cell toxicity, Amino Acids 46 (2014) 187–198.
[31] B. Jacob, G. Rajasekaran, E.Y. Kim, I.-S. Park, J.-K. Bang, S.Y. Shin, The stereochemical effect of SMAP-29 and SMAP-18 on bacterial selectivity, membrane interaction and anti-inflammatory activity, Amino Acids 48 (2016) 1241–1251.
[32] B.F. Tack, M.V. Sawai, W.R. Kearney, A.D. Robertson, M.A. Sherman, W. Wang, T. Hong, L.M. Boo, H. Wu, A.J. Waring, SMAP-29 has two LPS-binding sites and a central hinge, Eur. J. Biochem. 269 (4) (2002) 1181–1189.
[33] B. Jung, H. Yun, H.J. Min, S. Yang, S.Y. Shin, C.W. Lee, Discovery of structural and functional transition sites for membrane-penetrating activity of sheep myeloid antimicrobial peptide-18, Sci. Rep. 13 (1) (2023) 1238.
[34] P. Wayne, Clinical and laboratory standards institute (CLSI), Performance standards for antimicrobial susceptibility testing (2015).
[35] N. Radhakrishnan, S.D. Kumar, S.-Y. Shin, S. Yang, Enhancing selective antimicrobial and antibiofilm activities of melittin through 6-aminohexanoic acid substitution, Biomolecules 14 (6) (2024) 699.
[36] C. Ajish, S. Yang, S.D. Kumar, E.Y. Kim, H.J. Min, C.W. Lee, S.-H. Shin, S.Y. Shin, A novel hybrid peptide composed of LfcinB6 and KR-12-a4 with enhanced antimicrobial, anti-inflammatory and anti-biofilm activities, Sci. Rep. 12 (1) (2022) 4365.
[37] I. Jahan, S.D. Kumar, S.Y. Shin, C.W. Lee, S.-H. Shin, S. Yang, Multifunctional properties of BMAP-18 and its aliphatic analog against drug-resistant bacteria, Pharmaceuticals 16 (10) (2023) 1356.
[38] J.J. Harrison, C.A. Stremick, R.J. Turner, N.D. Allan, M.E. Olson, H. Ceri, Microtiter susceptibility testing of microbes growing on peg lids: a miniaturized biofilm model for high-throughput screening, Nat. Protoc. 5 (7) (2010) 1236–1254.
[39] A. Basak, Y. Abouelhassan, R. Zuo, H. Yousaf, Y. Ding, R.W. Huigens, Antimicrobial peptide-inspired NH125 analogues: bacterial and fungal biofilm-eradicating agents and rapid killers of MRSA persisters, Org. Biomol. Chem. 15 (26) (2017) 5503–5512.
[40] R. Bucki, K. Leszczyńska, A. Namiot, W. Sokołowski, Cathelicidin LL-37: a multitask antimicrobial peptide, Arch. Immunol. Ther. Exp. 58 (2010) 15–25.
[41] C.J. Miller, B.S. Drasar, R.G. Feachem, Response of toxigenic Vibrio cholerae 01 to physico-chemical stresses in aquatic environments, Epidemiol. Infect. 93 (3) (1984) 475–495.
[42] C.C. Häse, B. Barquera, Role of sodium bioenergetics in Vibrio cholerae, Biochimica et Biophysica Acta (BBA)-Bioenergetics 1505 (1) (2001) 169–178.
[43] H. Lee, S.I. Lim, S.-H. Shin, Y. Lim, J.W. Koh, S. Yang, Conjugation of cell-penetrating peptides to antimicrobial peptides enhances antibacterial activity, ACS Omega 4 (13) (2019) 15694–15701.
[44] H. Lee, S.-H. Shin, S. Yang, Rationally designed PMAP-23 derivatives with enhanced bactericidal and anticancer activity based on the molecular mechanism of peptide–membrane interactions, Amino Acids 55 (8) (2023) 1013–1022.
[45] H. Lee, S. Yang, S.-H. Shin, Effect of central PxxP motif in amphipathic alpha-helical peptides on antimicrobial activity and mode of action, Journal of Analytical Science and Technology 14 (1) (2023) 33.
[46] H. Lee, S. Yang, S.Y. Shin, Improved cell selectivity of symmetric α-helical peptides derived from trp-rich antimicrobial peptides, Bull. Kor. Chem. Soc. 41 (9) (2020) 930–936.

[47] S. Yang, C.W. Lee, H.J. Kim, H.-H. Jung, J.I. Kim, S.Y. Shin, S.-H. Shin, Structural analysis and mode of action of BMAP-27, a cathelicidin-derived antimicrobial peptide, Peptides 118 (2019) 170106.
[48] S.-T. Yang, S.-Y. Shin, S.-H. Shin, The central PXXP motif is crucial for PMAP-23 translocation across the lipid bilayer, Int. J. Mol. Sci. 22 (18) (2021) 9752.
[49] A.P. Galvao da Silva, D. Unks, S.-c. Lyu, J. Ma, R. Zbozien-Pacamaj, X. Chen, In vitro and in vivo antimicrobial activity of granulysin-derived peptides against Vibrio cholerae, Journal of antimicrobial chemotherapy (Print) 61 (5) (2008) 1103–1109.
[50] B. Das, J. Verma, P. Kumar, A. Ghosh, T. Ramamurthy, Antibiotic resistance in Vibrio cholerae: understanding the ecology of resistance genes and mechanisms, Vaccine 38 (2020) A83–A92.
[51] B.H. Gan, J. Gaynord, S.M. Rowe, T. Deingruber, D.R. Spring, The multifaceted nature of antimicrobial peptides: current synthetic chemistry approaches and future directions, Chem. Soc. Rev. 50 (13) (2021) 7820–7880.
[52] W. Li, F. Separovic, N.M. O'Brien-Simpson, J.D. Wade, Chemically modified and conjugated antimicrobial peptides against superbugs, Chem. Soc. Rev. 50 (8) (2021) 4932–4973.
[53] S. Xu, P. Tan, Q. Tang, T. Wang, Y. Ding, H. Fu, Y. Zhang, C. Zhou, M. Song, Q. Tang, Enhancing the stability of antimicrobial peptides: from design strategies to biomedical applications, Chem. Eng. J. (2023) 145923.
[54] H.-T. Chou, T.-Y. Kuo, J.-C. Chiang, M.-J. Pei, W.-T. Yang, H.-C. Yu, S.-B. Lin, W.-J. Chen, Design and synthesis of cationic antimicrobial peptides with improved activity and selectivity against Vibrio spp, Int. J. Antimicrob. Agents 32 (2) (2008) 130–138.
[55] S.M. Faruque, K. Biswas, S.N. Udden, Q.S. Ahmad, D.A. Sack, G.B. Nair, J.J. Mekalanos, Transmissibility of cholera: in vivo-formed biofilms and their relationship to infectivity and persistence in the environment, Proc. Natl. Acad. Sci. USA 103 (16) (2006) 6350–6355.
[56] F.H. Yildiz, K.L. Visick, Vibrio biofilms: so much the same yet so different, Trends Microbiol. 17 (3) (2009) 109–118.
[57] J.K. Teschler, C.D. Nadell, K. Drescher, F.H. Yildiz, Mechanisms underlying Vibrio cholerae biofilm formation and dispersion, Annu. Rev. Microbiol. 76 (1) (2022) 503–532.
[58] J.K. Teschler, D. Zamorano-Sánchez, A.S. Utada, C.J. Warner, G.C. Wong, R.G. Linington, F.H. Yildiz, Living in the matrix: assembly and control of Vibrio cholerae biofilms, Nat. Rev. Microbiol. 13 (5) (2015) 255–268.
[59] A.J. Silva, J.A. Benitez, Vibrio cholerae biofilms and cholera pathogenesis, PLoS Neglected Trop. Dis. 10 (2) (2016) e0004330.